Astron. Astrophys. 321, 323–329 (1997)

ASTRONOMY AND ASTROPHYSICS

Solar dynamics over cycle 19 using sunspots as tracers

E. Nesme-Ribes[1,⋆], **N. Meunier**[1], **and I. Vince**[2]

[1]URA 2080 CNRS, Département d'Astronomie Solaire et Planétaire, Observatoire de Paris, 5 Place Janssen, F-92195 Meudon, France

[2]Astronomical Observatory, Volgina 7, YU 11050 Beograd, Yugoslavia

Received 17 May 1996 / Accepted 1 October 1996

Abstract. The angular velocities and meridional motions of cycle 19 sunspots observed at Meudon were investigated. We compare our results with cycle 21 sunspot rotation properties (Nesme-Ribes et al. 1993a). We found also a complex latitudinal meridional circulation pattern similar to what was observed on cycle 21 sunspots (Nesme-Ribes et al. 1993b). We also corroborated the very small sunspot covariance (i.e. angular momentum transport via Reynolds stresses), which imposes a strong constraint on the source term of the differential rotation modeling.

Key words: sunspots – Sun: rotation – Sun: magnetic fields – Sun: activity

1. Introduction

Various tracers (particularly sunspots) have been used to characterize solar dynamics. Cycle 21 sunspots of Meudon K_{1v} spectroheliograms have been studied previously by Nesme-Ribes et al. (1993a; 1993b, referred to hereafter as Papers I and II, respectively), where their angular rotation and meridional motion were investigated. These reveal new sunspot properties, namely variable rotation through the solar cycle and a very small latitudinal angular momentum transport via Reynolds stresses. However, these authors also found some net meridional circulation, which could contribute to maintaining the observed differential rotation.

The present work consists in extending the above previous studies to cycle 19 sunspots. Our aim was first to confirm or refute the properties detected in Papers I and II, and secondly to determine the time-variability of the azimuthal field: cycle 19 was the most active since Galileo's time. Our result will be compared extensively to cycle 21 sunspot properties.

Observational data are presented in Sect. 2, the angular velocity is discussed in Sect. 3, and the meridional circulation in Sect. 4. The correlation between these two motions (the "covariance") is calculated in Sect. 5, in order to estimate the Reynolds stress contribution to angular momentum transport, which is a question related to the origin of the differential rotation.

Send offprint requests to: N. Meunier

⋆ Deceased on November the 25th, 1996

Table 1. Sunspot number in the Meudon sample

Year	N. Hemisphere	S. Hemisphere	Total
1957	181	188	369
1958	273	257	530
1959	647	206	853
1960	252	180	432
1961	161	67	228
1962	24	6	30
1957-1962	1538	904	2442

2. Observational data

Sunspots are tracked on the Meudon K_{1v} spectroheliograms (1.5 Å off the Ca II K line center), which display faculae and sunspots at the photospheric level, about 500 km above the $\tau = 1$ level. The images have been digitized with 1.8 arcsec resolution, which corresponds to the average spatial resolution obtained at Meudon. Image processing and tracking procedures are described and discussed at length in Mein & Ribes (1990) and in Paper I. The random error on each sunspot velocity measurement is of the order of 15 m/s. The number of sunspots per hemisphere and per year, and for the whole period, is shown in Table 1.

3. Angular rotation rate

3.1. Global rotation

The differential rotation rate is calculated for each 5° latitude bin and is plotted in Fig. 1, along with the 1-σ deviation from the mean. These deviations are of the order of 0.04°/day. The rotation appears rigid over a broad range of latitudes. This rigidity may be due to a deep anchoring of young sunspots, if we may indeed assume such is the case, because our tracking procedure preferentially selects these young sunspots. To compare with other data, we began by performing a fourth-degree Legendre polynomial fit, using a least-squares minimization of the observed data, averaged over 5° latitude bins. Since we observed

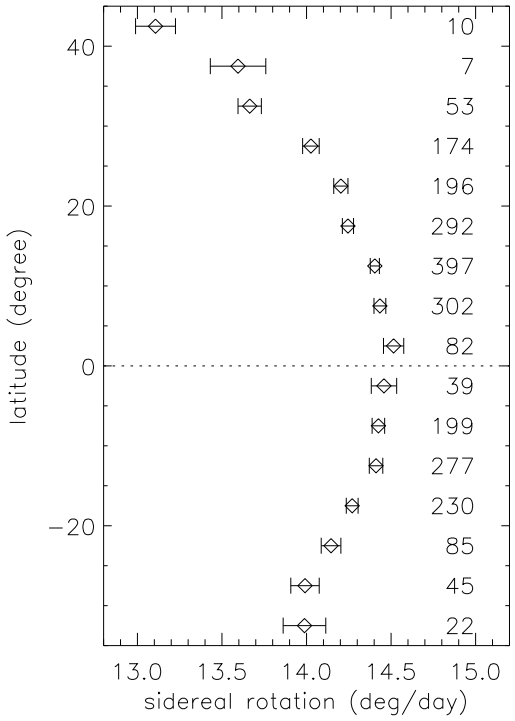

Fig. 1. Sidereal rotation rate of Meudon sunspot data, in 5° latitude bins, for the period 1957 to 1962. Errors are at the 1-σ confidence level

no strong north-south asymmetry in rotation rates, we kept only the even Legendre coefficients, which are then converted to A, B, and C, such that the rotation rate is modeled by

$$\Omega(\theta) = A + B\sin^2\theta + C\sin^4\theta, \quad (1)$$

where θ is the latitude. Fig. 2 compares the polynomial fit performed on cycle 19 and 21 sunspots. The rotation during cycle 21 seems to be a little more rigid than that of cycle 19, and exhibits a slightly smaller equatorial rotation rate, though the differences are not significant. This rigidity has also been observed by Antonucci et al. (1990) on large-scale photospheric features.

3.2. Cycle variability

We now investigate the variability of the rotation rate throughout the cycle. Table 2 shows the expansion (1) coefficients during cycle 19. The period ranging from 1957 to 1959 is one of intense activity, while the minimum occurred in 1963. Errors at the 1-σ confidence level are computed using a Monte Carlo simulation.

The errors in the Legendre polynomial coefficients are usually determined by computing the covariance matrix (see Press et al. 1986, p521ff). However, this method assumes that when the fit parameters are displaced from their optimum values by a deviation

$$\mathbf{a} \equiv (a_1, a_2, ..., a_M), \quad (2)$$

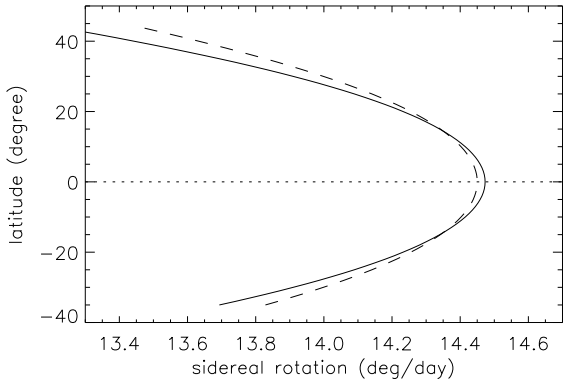

Fig. 2. Comparison of cycle 19 (solid line) and 21 (dashed line) sunspot rotation rates using a fourth-degree polynomial fit on the averaged data

Table 2. Parameters of expansion $\Omega(\theta) = A + B\sin^2\theta + C\sin^4\theta$, where θ is the latitude, for cycle 19 sunspots (in μrad/s) and cycle 21 (Paper I). Errors are at the 1-σ confidence level

Year	A	σ_A	B	σ_B	C	σ_C
Cycle 21	2.921	0.017	-0.42	0.36	0.10	1.29
1957	2.932	0.047	-0.38	0.84	-0.44	2.64
1958	2.910	0.019	-0.30	0.21	-1.15	1.30
1959	2.937	0.026	-0.59	0.55	-0.02	2.35
1960	2.910	0.023	-0.26	0.55	0.11	2.15
1961	2.928	0.006	0.30	0.27	-8.92	1.95
1957-1962	2.924	0.013	-0.38	0.20	-0.30	0.71

then the resulting deviation in χ^2 is quadratic:

$$\chi^2(\mathbf{a}) \sim \chi^2(\mathbf{0}) + \frac{1}{2}\sum_{j,k=1}^{M} D_{jk}a_j a_k. \quad (3)$$

When higher order terms are significant, the covariance matrix becomes unreliable, and we turn to Monte Carlo simulations to estimate realistic errors (Press et al. 1986, p529ff). We found that errors computed with the two methods are different, so we adopted the Monte Carlo method to determine them.

Based on these errors, we conclude that the variations of the coefficients A, B, and C over the five year duration of the data set were not significant.

3.3. North-south asymmetry

To investigate the north-south asymmetry of sunspot rotation rates, we now consider the odd coefficients of the polynomial expansion

$$\Omega(\theta) = \sum_{i=0}^{i=4} A_i \sin^i\theta, \quad (4)$$

where A_0, A_2, and A_4 are the coefficients A, B, and C of Eq. 1. A_1 and A_3 represent the north-south asymmetry of the rotation rate at low and high latitudes, respectively. A_1 and A_3 are shown

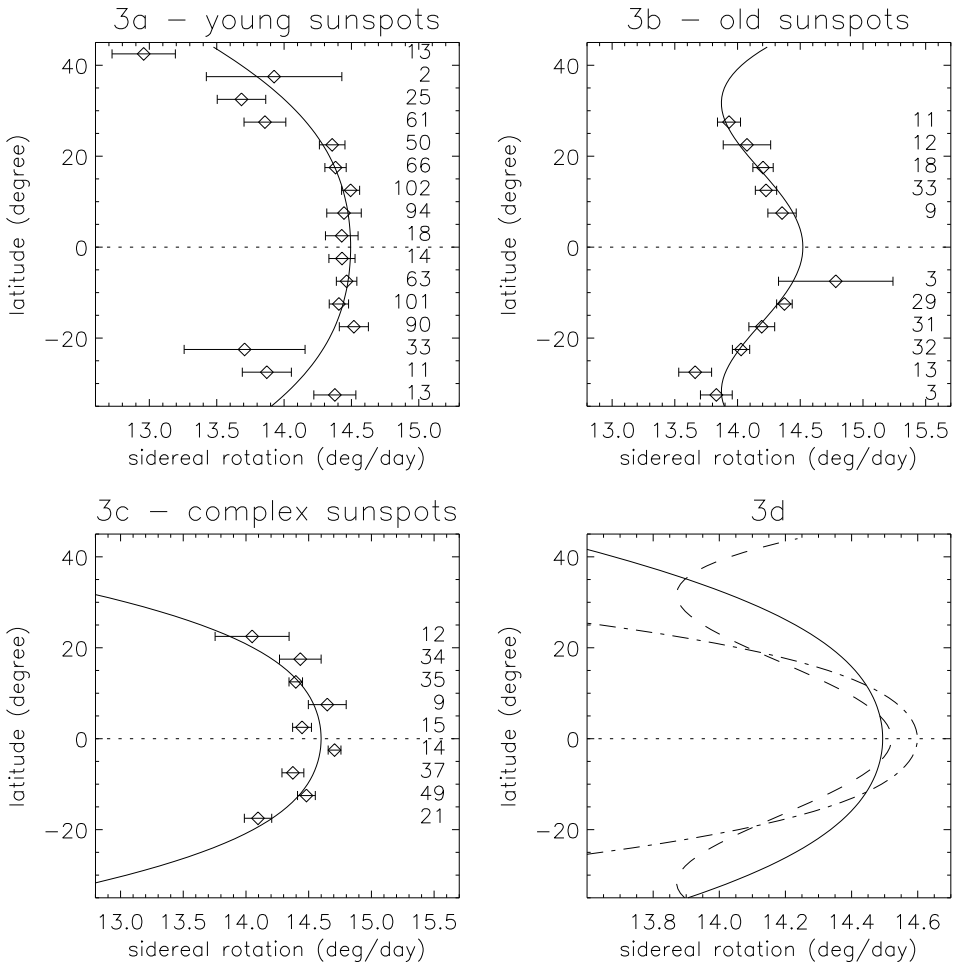

Fig. 3. Sidereal rotation rate of cycle 19 Meudon sunspots, according to age. Top left: sunspots younger than 4 days. Top right: sunspots older than 8 days. Bottom left: complex sunspots. Bottom right: polynomial fits for young (solid line), old (dashed line), and complex (dotted line) sunspots. Error bars are at the 1-σ confidence level

Table 3. North-south asymmetry coefficients for cycle 19 and 21, with their 1-σ errors

Year	A_1	σ_1	A_3	σ_3
19	0.086	0.238	-0.707	1.522
21	-0.171	0.348	0.735	2.168

in Table 3 for cycles 19 and 21. Let us note that A_3 is not reliable because there are too few sunspots at high latitudes, but a second-degree polynomial fit would provide a poor fit of the data. Both cycles exhibit no significant north-south asymmetry.

3.4. Age and magnetic polarity dependence

We then examined the variability of the rotation rates with sunspot age. For this purpose, two classes of sunspots were considered: those four days old or less (759 sunspots) and those more than eight days old (194 sunspots). We also considered "complex sunspot" rotation rates. Complex sunspots belong to groups in which it is not possible to determine their age. Fig. 3.2 shows the rotation rates for the three classes and compares their respective polynomial fits. Young sunspots show a slightly more rigid rotation than old ones. The uncertainty on the coefficients A, B and C are large, due to the small sampling. However, the same trend was observed in cycle 21 sunspots, which gives some confidence in the result. It should be noted that other sunspot data sets (Mount Wilson) and sunspot-group data sets (Greenwich) also show that sunspots rotation is age-dependent (e.g. Ward, 1965; Gilman & Howard, 1983). However, these authors could not conclude that young sunspots were deeply anchored: the rigidity of young sunspot rotation suggests a deep anchorage, at a place where the convective layers show little differential rotation.

A bipolar group consists of a pair of sunspots of opposite polarity, with one leading and one following. The rotation rates of leaders (432 points) and followers (175 points) is studied separately (Fig. 3.4). However, the error bars are too large to detect any significant differences between these two sunspot classes, as the one observed by Gilman & Howard (1985) and in Paper II (faster rotation of leaders).

4. Meridional circulation

4.1. Net meridional circulation

We calculated the meridional circulation (referred to hereafter as "m.c.") of cycle 19 sunspots (Fig. 5). Our convention is a

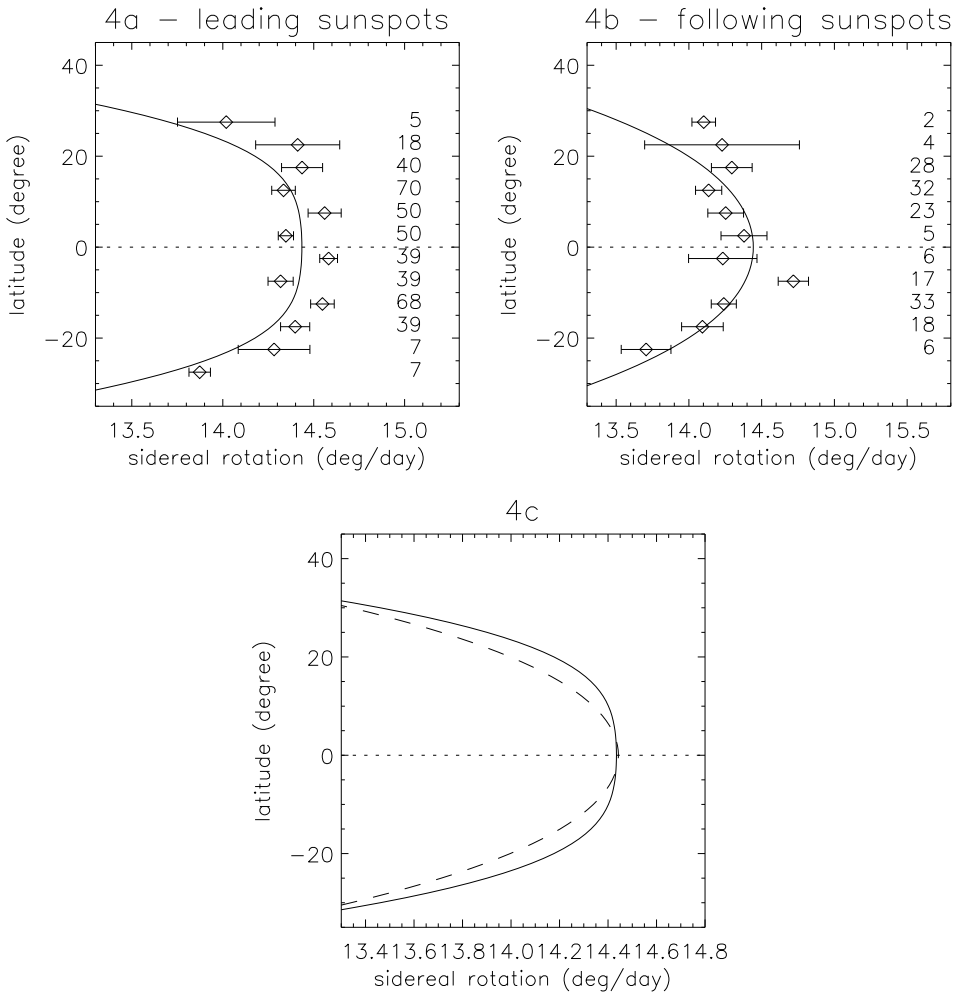

Fig. 4. Sidereal rotation rate of cycle 19 Meudon leading and following sunspots. Top left: leaders. Top right: followers. Bottom: polynomial fit for leaders (solid line) and followers (dashed line). Error bars are at the 1-σ confidence level

positive m.c. towards the North pole. The observed motions are equatorward at low latitudes (though hardly significant) and poleward at high latitudes, for both cycles. For comparison, net m.c. for cycle 21 is also shown. The m.c. pattern is more pronounced for cycle 19 sunspots, particularly in the case of low-latitude sunspots.

We considered the averaged m.c. per hemisphere for the whole cycle. We obtained $0.005\pm0.010°$/day for the northern hemisphere and $0.016\pm0.011°$/day for the southern hemisphere. These averages are hardly significant, because the pattern is latitude-dependent, directed toward one or the other pole. For this reason, it is not possible to use these averages to investigate the cycle variability of m.c. in detail.

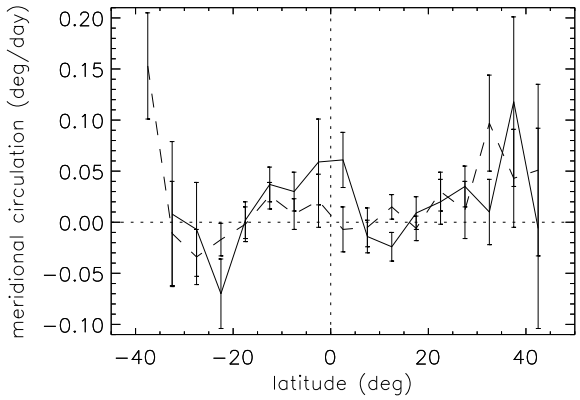

Fig. 5. Meridional circulation of cycle 19 (solid line) and cycle 21 (dashed line) sunspots. Error bars for cycle 19 are at the 1-σ confidence level

5. Reynolds stresses

In this section, we address the important question of the angular momentum transport, which is related to the origin of the differential rotation. Let us use u and v to denote the latitudinal and longitudinal motions, respectively. The m.c. u is now positive when equatorward in both hemispheres. The transport of linear angular momentum across a given latitude circle (Ward 1965) is proportional to

$$< [uv] >=< [u] >< [v] > + < [u]^*[v]^* > + < [u^\bullet v^\bullet] >, \quad (5)$$

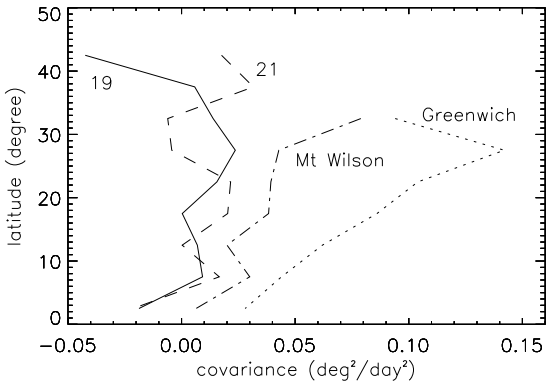

Fig. 6. Sunspot covariance during cycle 19 (Meudon, solid line), cycle 21 (Meudon, dashed line), Mount Wilson sunspots (1921-1982, dot-dashed line) and Greenwich sunspots (1925-1954, dotted line)

where [ ] indicate spatial averages and $^\bullet$ spatial deviations from this average; $< >$ indicate time averages and $[\ ]^*$ are deviations from the time-space average. The first term, $< [u] >< [v] >$, represents the transport by the meridional flow (hereafter "M.C.T."). The second and third terms represent the transport by non-axisymmetrical eddies. We cannot separate these but they measure the correlation between the two horizontal motions

$$< [u]^*[v]^* > + < [u^\bullet v^\bullet] >=< [u'v'] >=$$

$$< [(u- < [u] >)(v- < [v] >)] > . \quad (6)$$

This correlation (or "covariance") term is a measure of the latitudinal angular momentum transport via Reynolds stresses. Positive covariance implies that higher-than-average longitudinal motion in the direction of rotation is coupled with equatorward motion (see Paper II for more details).

5.1. Covariance of cycle 19 sunspots

The covariance has been calculated within each 5° latitude bin, and for all cycle 19 Meudon sunspots (Table 4). The covariance is found to be very small and mainly positive, in the northern hemisphere, while negative in the southern. Fig. 6 shows the covariance obtained for all cycle 19 sunspots. The two hemispheres have been folded. We observe a very small covariance (less than 0.02 $(\mathrm{deg/day})^2$). As previously noted in Sect. 4, there seems to be a very small contribution to the equatorial acceleration at low latitudes and to poleward acceleration at high latitudes. Our results are in agreement with those for cycle 21 sunspots (Paper II), unlike those of the Mount Wilson analysis (Gilman & Howard 1984) and Greenwich sunspot groups (Ward 1965).

We also compare the covariance between cycle 19 and 21 sunspots for each hemisphere, separately, in Fig. 5.1. In each case, the covariance is of the same order of magnitude. The observed differences between the two hemispheres are within the noise level.

5.2. Leading and following sunspot covariance

Considering now whether the covariance varies with sunspot polarity and age, we take the covariance for leading and following sunspots shown in Fig. 8. The two hemispheres have been folded. Leaders seem to exhibit a higher covariance than followers (positive for leaders and negative for followers). This is probably due to the tilt angle of the emerging bipolar group.

5.3. Old/young sunspot covariance

Fig. 9 displays young and old sunspot covariances for cycle 19. We observed no strong difference between the two sunspot classes. This does not confirm the higher covariance for young sunspots as detected in Paper II. The difference in covariance between leading and following sunspots and between old and young sunspots is probably not significant. The robust result is that sunspots do not show much significant transport via Reynolds stresses.

6. Conclusion

In this paper, we investigated cycle 19 sunspot dynamics from Meudon spectroheliograms and compared this with cycle 21 sunspot properties obtained by a similar method (Papers I and II).

Angular rotation rates exhibit no significant variation over the five years of the data set. We did not detect any strong north-south asymmetry in rotation rates in either the cycle 19 or 21 sunspots.

Our m.c. study confirms cycle 21 sunspot results (Paper II), namely a poleward/equatorward m.c. pattern with latitude-dependence. We also computed sunspot covariance and found it to be very small. The differences observed in Paper II between leader and follower behaviors, and between old and young sunspots, are not present in cycle 19, and probably reflect some internal variability specific to cycle 21. So the main conclusion of this paper together with Paper II is the following. The covariance exhibited by sunspots seems to be very small. Recent modeling of the differential rotation (Küker et al. 1993) requires a smaller covariance than previous models, which would be in agreement with our observations. A discussion of these results as well as facula covariances is given in Meunier et al. (1996b).

Two main sunspot data sets are available for the same period (cycle 19): the Greenwich photoheliographic plates and the Mount Wilson observations. The rotation obtained from these data sets agrees fairly well with the Meudon sunspot rotation. However, there are strong discrepancies in the covariances. The Greenwich covariance was calculated from the motions of the barycenter of the whole sunspot groups (Ward, 1965; Balthasar et al., 1986). So a direct comparison with individual sunspot motions is not straightforward, as discussed at length in Paper I. The motions of individual sunspots are available from the Mount Wilson data set. However, the tracking procedure used by Howard et al. (1984) is subject to biases mentioned in Papers I and II.

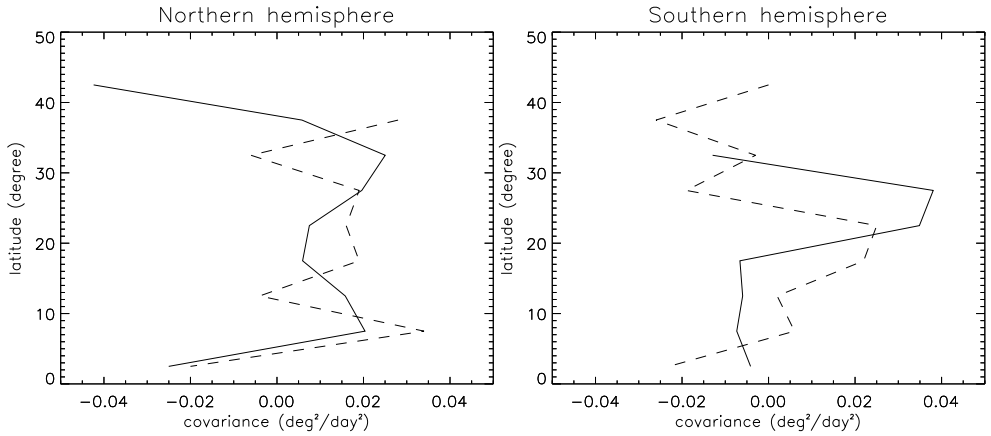

Fig. 7. Meudon sunspot covariance during cycles 19 (solid line) and 21 (dashed line). Left: northern hemisphere. Right: southern hemisphere

Table 4. Angular momentum transport by Reynolds stresses and by meridional flow, for the whole period (1957-1962). Positive covariance implies that higher-than-average longitudinal motion in the direction of rotation is coupled with equatorward motion

Northern Hemisphere (1957-1962)									
Latitude	42.5°	37.5°	32.5°	27.5°	22.5°	17.5°	12.5°	7.5°	2.5°
Covariance	-0.042	0.006	0.025	0.020	0.007	0.006	0..016	0.020	-0.025
M. C. T.	0.079	-1.604	-0.137	-0.491	-0.284	-0.128	0.346	0.202	-0.885
Southern Hemisphere (1957-1962)									
Latitude	42.5°	37.5°	32.5°	27.5°	22.5°	17.5°	12.5°	7.5°	2.5°
Covariance	-	-	-0.013	0.038	0.035	-0.007	-0.006	-0.007	-0.004
M. C. T.	-	-	0.112	-0.098	-0.990	0.028	0.533	0.433	0.853

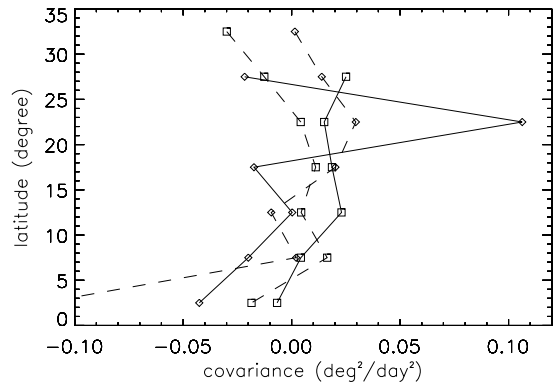

Fig. 8. Covariance of leading (□) and following (◇) sunspots during cycles 19 (1957-1962, solid line) and 21 (1977-1984, dashed line) from Meudon data

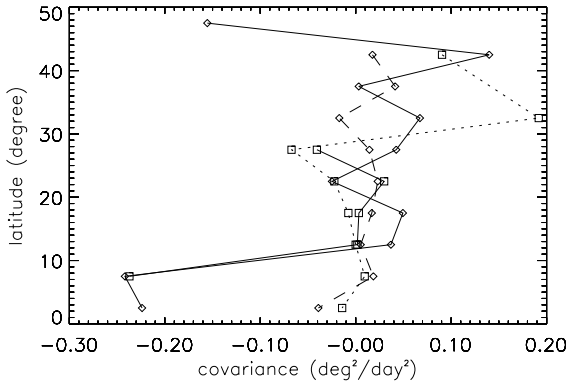

Fig. 9. Covariance of young (□) and old (◇) sunspots during cycles 19 (1957-1962, solid line) and 21 (1977-1984, dashed line: young sunspots and dotted line: old sunspots) from Meudon data

In Collin et al. (1995), we used helioseismology results (Gough et al. 1993) to deduce tracer anchorage depth. In the present work, we obtain similar rotation rates for old and young sunspots, so we confirm our conclusion about the deep sunspot anchorage. However, seismic observations of internal rotation are not available for cycle 19, and it might be unsafe to extrapolate cycle 21 data to cycle 19.

Acknowledgements. One of us (E. Nesme) is grateful to the Ministery of Defense, for encouraging and funding the long-term spectroheliogram research program, through military contracts (no. 010481/ETCA, no. 012736/DRET-ETCA, and no. 92-2011.A/DRET-ETCA). The extensive work of the spectroheliogram observations team has been crucial for almost a century. We thank the present team for maintaining and improving the observational program over the years. Spectroheliograms were digitized with the *Machine à Mesurer pour l'Astronomie* (MAMA) of the Institut National des Sciences de l'Univers, at the Paris Observatory. Our thanks also go to P. Micheneau, R. Chesnel, and P. Toupet for their assistance in the data acquisition.

References

Antonucci E., Hoeksema J.T. & Scherrer P.H., 1990, ApJ 360, 296
Balthasar H., Vázquez M. & Wöhl H., 1986, A&A 155, 87
Collin B., Nesme-Ribes E., Leroy B., Meunier N. & Sokoloff D., 1995, C. R. Acad. Sci., Paris, t. 321, Série IIb, 111
Gilman P.A. & Howard R., 1984, Sol. Phys. 93, 171
Gilman P.A. & Howard R., 1985, ApJ 295, 233
Gough D.O., Kosovichev A.G., Sekii T., Librecht K.G. & Woodard M.F., 1993, in: A. Baglin & W. Weiss (eds.), Proceeding IAU Coll. 137, 93
Küker M., Rüdiger G. & Kitchatinov L.L., 1993, A&A 279, L1
Mein P. & Ribes E., 1990, A&A 227, 577
Meunier N., Nesme-Ribes E. & Grosso N., 1996a, accepted in A&A (in press)
Meunier N., Nesme-Ribes E. & Collin B., 1996b, accepted in A&A (in press)
Nesme-Ribes E., Ferreira E.N. & Mein P., 1993a, A&A 274, 563 (Paper I)
Nesme-Ribes E., Ferreira E.N. & Vince I., 1993b, A&A 276, 211 (Paper II)
Press W.H., Flannery B.P., Teukolsky S.A. & Vetterling W.T., 1986, Numerical Recipes, Cambridge University Press
Ward F., 1965, ApJ 141, 534

This article was processed by the author using Springer-Verlag LaTeX A&A style file *L-AA* version 3.